

Balancing Biases and Preserving Privacy on Balanced Faces in the Wild

Joseph P Robinson, *Student Member, IEEE*, Can Qin, *Student Member, IEEE*, Yann Henon, Samson Timoner, and Yun Fu, *Fellow, IEEE*

Abstract—There are demographic biases in the SOTA CNN used for FR. Our BFW dataset serves as a proxy to measure bias across ethnicity and gender subgroups, allowing us to characterize FR performances per subgroup. We show performances are non-optimal when a single score threshold is used to determine whether sample pairs are *genuine* or *imposter*. Furthermore, actual performance ratings vary greatly from the reported across subgroups. Thus, claims of specific error rates only hold true for populations matching that of the validation data. We mitigate the imbalanced performances using a novel domain adaptation learning scheme on the facial encodings extracted using SOTA deep nets. Not only does this technique balance performance, but it also boosts the overall performance. A benefit of the proposed is to preserve identity information in facial features while removing demographic knowledge in the lower dimensional features. The removal of demographic knowledge prevents future potential biases from being injected into decision making. Additionally, privacy concerns are satisfied by this removal. We explore why this works qualitatively with hard samples. We also show quantitatively that subgroup classifiers can no longer learn from the encodings mapped by the proposed.

Index Terms—Facial recognition, Fair ML, Bias in AI, Balanced dataset, Imbalanced data problem.



1 INTRODUCTION

THE more our society becomes integrated with machine learning (ML), the higher the interest in topics such as bias, fairness, and even the implications for the underlying formalization of existing or prospective ML standards [1]–[3]. A common trend in both research and mainstream has grown clear: the more we depend on technology that accelerates or automates everyday tasks, the more attention concepts such as biased and unfair algorithms should receive [4]. Furthermore, systems deployed for sensitive tasks, such as biometrics [5] (*e.g.*, facial recognition (FR)), need to be fully considered and understood. The perspective here recognizes the tendency of the researcher, the reporter, and the consumer to maintain transparency.

In FR, a typical model is trained on large-scale, paired face data, and then deployed for some flavor of facial verification (FV) - a boolean matching function (Fig. 1). Today, models tend to be convolutional neural networks (CNNs) and trained to encode faces - the goal is to represent faces from an N-dimensional space with minimal distances between samples of the same identity and maximum between different identities. Hence, the aim is to discriminate between subjects from the face encodings.

Now, provided two or more faces features encoded by a CNN, a distance (or similarity score) s must be learned such to act as a decision boundary to separate the genuine pairs score from the imposters score. Ideally, genuine and imposter scores would be completely separable. However, this is not the case in practice. It is this score-threshold (*i.e.*, θ) that determines whether or not the pair should be accepted. The implications are for faces features: to be assumed as the same, genuine class the score (or distance) must satisfy a criterion in the form of a single value [6]–[9].

Mathematically, the decision D in similarity space is defined as

$$D = \begin{cases} \text{accept} & \text{if } s \geq \theta \\ \text{reject} & \text{if } s < \theta \end{cases}$$

The importance of θ should not be overlooked - a hyperparameter that is a decision boundary in metric space. The optimal value depends on the specific use-case (*i.e.*, larger thresholds yield a lower probability that a sample is predicted as a true match). Regardless, the choice in threshold has a clear trade-off between false-positive (FP) and false-negative (FN) rates. For instance, a system that is claimed to perform at an error rate of 1 and 10,000, *i.e.*, one in every ten-thousand instances are incorrectly matched. We would then set our system by determining the threshold based on held-out data samples that allow the desired target error rate to be matched (Fig. 2). The problem, per convention, is which assumes an average result across a held-out that then only holds true on the distribution of the source used. Then, specific cohorts (*e.g.*, ethnicity, gender, and other demographics) are unequally weighted due to an unequal representation. So, that single, global threshold, which is a sort of crude measure to begin with, is skewed to different cohorts that are not fairly represented by the source. In the end, these systems favor some demographics over others, and it is the bias for which a change in cohort causes a change in the average performance of an algorithm.

The adverse effects of a global threshold are three-fold: (1) the evaluation set is typically imbalanced. The demographics of the majority are weighted more in the reported performance ratings. Therefore, reported results skew to rarer traits that are more common in the underrepresented subgroups— a phenomena that should be considered for different subgroups (*i.e.*, gender, ethnicity, race, age). (2) the mappings produced by a CNN have various levels of sensitivity in the metric (Fig. 3). Therefore, the range of distances between true pairs varies across demographics. (3) a global threshold is referenced when

• J.P. Robinson, C. Qin, and Y. Fu are with the College of Engineering, Northeastern University, Boston, MA, 02115.

• Y. Hann and S. Timoner are with ISM, Cambridge, MA, 02138.

Manuscript submitted November 2, 2020.

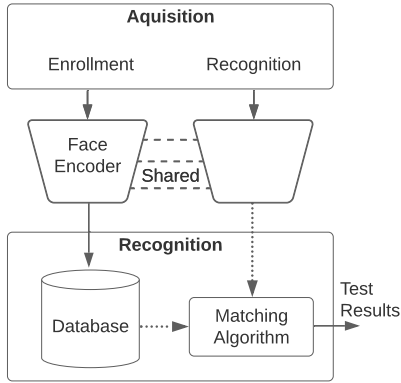


Fig. 1: **Generic recognition system.** Faces are often stored as encodings in a database through *enrollment*. *Recognition* is then to compare the encoding of an input face to those in the database.

comparing face encodings. Since the optimal score shifts for different demographics, there ought to be variable thresholds (*i.e.*, sliding threshold set according to demographic information). Furthermore, the validation set used to determine global threshold and the test set used to report results should be understood - this issue will be unnoticed in performance ratings if the validation and test are from the same distribution and, thus, the resulting performance ratings are based in favor of the majority. This leads to performance ratings that are incomplete and even misleading.

To address the lack of a balanced data (*i.e.*, (1)), we propose to evaluate on our dataset, which was built specifically for measuring biases in demographics for FV systems in a systematic, reproducible way. With it, we introduce a new benchmark for FR, called Balanced Faces In the Wild (BFW) (Fig. 4). BFW serves as a platform to fairly evaluate FR systems and enable demographic-specific ratings to be reported (Table 1). We use BFW to gain a deeper understanding of the extent of bias present in facial embeddings extracted from a state-of-the-art (SOTA) CNN model. We then suggest a mechanism to counter the biased feature space to mitigate problems of bias with more balanced performance ratings across demographics, and all the while improving the overall accuracy. Specifically, we unlearn demographic knowledge in face encodings, while preserving identity information. Thus, we learn to map the encodings to a lower dimensional space containing less knowledge of subgroups. The byproducts are then embeddings that preserve the privacy of its subject’s ethnicity and gender (*i.e.*, subgroups). It is this feature adaptation scheme proposed to address items (2-3).

The contributions of this extension of [10] are the following:

- Demonstrate a bias in an existing SOTA CNN with our BFW dataset (Table 2). We propose a feature learning scheme that employs domain adaptation to debias face encodings and, most importantly, balances performances across subgroups such that the overall rating also greatly boosts.
- Hide attribute information in encodings— a byproduct of the proposed debiasing scheme is in the reduction of knowledge for attributes. Beyond privacy, it removes potential for others biases, whether unintended (*e.g.*, models trained on top) or intended bias (*e.g.*, human consciously using).
- Provide insights with analysis of hard samples overcome by the proposed debiasing scheme. Evidence in the form of salience mapping and face pairs are shown and discussed.

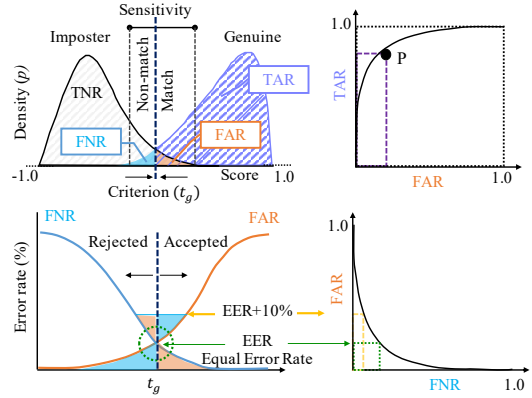


Fig. 2: **Depiction of biometrics.** The signal detection model (SDM) shows the sensitivity related to a single threshold t_g (*top-left*). The area to the right of the threshold considers all accepted pairs, both correctly and incorrectly predicted. True Acceptance Rate (TAR) as a function of False Acceptance Rate (FAR) is a common way to report ratings for given false-rates (*top-right*). Equally common in FR is the trade-off between false-negative rate (FNR) and FAR (*bottom-left* and *bottom-right*).

The rest of the paper is organized as follows. In Section 2, we review related work. We then cover our BFW database in Section 3. Then, in Section 4, we introduce the proposed methodology. Section 5 follows this with settings and results of the experiments, along with the details of our BFW database. Finally, we conclude and discuss next steps in Section 6.

2 RELATED WORK

We next review the related research. Specifically, we discuss modern-day FR systems (*i.e.*, SOTA neural network (NN)-based), along with the benchmark datasets for which these data-driven frameworks are trained. We follow this with a brief discussion on the supporting data focused on balance across label types. Then, we describe several related works in domain adaptation. Finally, we cover problems of privacy in FR.

2.1 Bias in FR

Modern-day deep models have worked with prominence in automatic face understanding problems. In 2014 Taigman *et al.* of Facebook first proposed using a deep CNN for FR [11]. Over a half of a decade later there has been at least one major contribution in conventional FR each year ever since (*i.e.*, 2015 [12], 2016 [13], 2017 [7], 2018 [6], 2019 [14], and even 2020, the year of facial masks [15]). Details on deep learning advances in FR technology are provided as a part of recent surveys [16], [17]; with another focused on bias specific to FR [18].

Biases in FR focus on characterizing performance across various *soft attributes*, such as gender, ethnicity, or age [5]. Researchers have spent great efforts proposing problem statements and solutions to problems of bias in FR technology. We focus on the demographics (or subgroups) of gender and ethnicity. The inherent problems here are two-fold. First, gender is handled as a boolean label, which is a gross approximation of individual uniqueness in question of sexuality - a spectrum of real numbers would be more appropriate [19]. Secondly, the definitions of race and ethnicity are loosely defined. The US Census Bureau allows

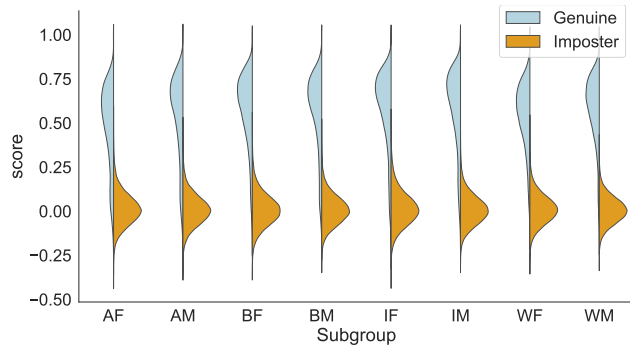


Fig. 3: **SDM across subgroups.** Scores of *imposters* have medians ≈ 0.3 but with variations in upper percentiles; *genuine* pairs vary in mean and spread (e.g., AF has more area of overlap). A threshold varying across different subgroups yields a constant FAR.

an individual to self-identify race.¹ We define it as a group of people having facial characteristics similar to those found in a region. The result is various types of biases in FR systems in favor of or against particular demographics remain a question.

Balakrishnan *et al.* trained a generator to manipulate latent space features in that the controlled attributes were skin-tone, length of hair, and hair color [20]. Another synthesis solution proposed was to generate faces across various ages as a means to augment training data [21]. Terhorst *et al.* recognized the same phenomena our work is found on—the variation in sensitivities of scores for different demographics [22]. Specifically, the authors propose a score normalization scheme to handle the problem of inaccurate performance ratings when demographic-specific performances are compared to the average—a problem highlighted in our conference paper [10], and is further extended in this paper.

Some aim to characterize the amount of bias in a system, whether it be for gender [23]–[25], ethnicity, age [26], or two or more of the aforementioned [27]–[31]. A recent *European Conference on Computer Vision* (ECCV) challenge provided incentive and for researchers to propose solutions for problems of bias with respect to ethnicity, gender, age, pose, and with and without sunglasses [32]. Other recent works in face recognition (FR) technology introduce additional modalities, such as profile information, to the problem of bias [33], [34]. Another research question concerns the measuring of biases in FR systems [23], [28]. Some focus on templates [35]. Some debias at the score level [22]. Some focus to debias pre-trained models [36]. Wang *et al.* introduced a reinforcement learning-based race balance network (RL-RBN) to find optimal margins for non-Caucasians as a Markov decision process before passing to the deep model that learns policies for an agent to select margins as an approximation of the Q-value function; *i.e.*, the skewness of feature scatter between races can be reduced [37]. Even more HCI-based views have been introduced as semi-supervised bias detection systems that act as tools with humans in-the-loop [38].

2.2 Imbalanced data and data problems in FR

The impact from the quality of fairness depends on the context for which it is used. Furthermore, various paradigms have been proposed as means to a solution: some alter the data distribution to yield classifiers of equal performances for all classes (*i.e.*,

re-sampling, like by under-sampling and over-sampling [39]); others alter the data itself (*i.e.*, algorithms that adjust classification costs). For instance, Oquab *et al.* re-sampled at the image patch-level [40]. Specifically, the aim was to balance foregrounds and backgrounds for object recognition. On the other hand, Rudd *et al.* proposed the mixed objective optimization network (MOON) architecture [41] that learns to classify attributes of faces by treating the problem as a multi-task (*i.e.*, a task per attribute) attribute to more balanced performances when training on data that has an imbalanced distribution across attributes. The Cluster-based Large Margin Local Embedding (CLMLE) [42] sampled clusters of samples in the feature-space that were used to regularize the models at the decision boundaries of underrepresented classes. See literature reviews for details on approaches that alter at the data or algorithmic-level [43]–[45].

More specific to faces, Drozdowski *et al.* summarizes that the cohorts of concern in biometrics are demographic (e.g., sex, age, and race), person-specific (e.g., pose or expression [46], and accessories like eye-wear or makeup), and environmental (e.g., camera-model, sensor size, illumination, occlusion) [5]. Albiero *et al.* found empirical support that having training data that is well balanced in gender does not mean that results of a gender-balanced test set will be balanced [47]. Our studies focus on the effect demographic has in FV by assessing demographic-specific classification ratings. Our BFW data resource allows us to analyze existing SOTA deep CNNs on different demographics (or subgroups). We provide insight in practical; experimental settings often report performance ratings that are misleading—ratings are dependent on the demographics of the population.

To match the capacity of modern-day deep models several large FR datasets were released [48]–[51]. More recently, several have reported on the imbalance in demographics are the data, and proposed balanced resources for FR-based tasks [3], [19], [52], [53]. Diversity in Faces (DiF) came first [19], which did not include identity labels. Moreover, DiF is no longer available for download. Others released data with demographics balanced, but for the task of predicting the demographic and, thus, do not include identity labels [3], [53]. Hupont *et al.* proposed DemogPairs is balanced across 6 subgroups of 600 identities from CASIA-WebFace (CASIA-W) [54], VGG [49], and VGG2 [50]. Similar to DemogPairs, except with 8 subgroups, 800 identities, and with number of faces per identity the same for all, our BFW data was the latest release for measuring bias in FR technology. Furthermore, recognizing that existing SOTA models are already trained on a public resource, we built BFW from just VGG2 to minimize conflicts in overlap between train and test. Table 1 compares our data with the others.

2.3 Feature Alignment / Domain Adaptation

Domain adaptation (DA) [55]–[57] employs labeled data from the source domain to make it generalize well to the typically label-scarce target domain; hence, a common solution to relieve annotation costs. DA can be roughly classified as the semi-supervised DA [57] or the unsupervised one [58] according to the access to target labels. The crucial challenge toward DA is the distribution shift of features across domains (*i.e.*, domain gap), which violates the distribution-sharing assumption of conventional machine learning problems. In our case, the different domains are the different subgroups (Table 2).

To bridge such gap, some of Feature Alignment (FA) methods attempt to project the raw data into a shared subspace

1. <https://www.census.gov>

where certain feature divergence or distance is minimized to confuse them. Various methods, such as Correlation Alignment (CORAL) [59], Maximum Mean Discrepancy (MMD) [60], and Geodesic Flow Kernel (GFK) [61], [62], have been developed in this line. Currently, adversarial domain alignment methods (*i.e.*, DANN [63], ADDA [64]) have attracted increasing attention by designing a zero-sum game between a domain classifier (*i.e.*, discriminator) and a feature generator. The features of different domains will be mixed if the discriminator cannot differentiate the source and target features. More recently, learning well-clustered target features proved to be helpful in conditional distributions alignment. Both DIRT-T [58] and MME [57] methods applied entropy loss on target features to implicitly group them as multiple clusters in the feature space to keep the discriminative structures through adaptation. Inspired by FA, we aim to align the score distributions of the different subgroups by adjusting the sensitivities in true scores (Fig. 3).

2.4 Protecting demographic information in FR

ML is growing more accessible. As such, it grows more in our day-to-day lives. The levels of sensitivities of the use-case ought to be put under careful consideration - not only the model, but the data too [65]. That means, intermediate results, also known as features are included. FR is an ML problem that has made great progress in recent years, being used *off-the-shelf* in many applications. It is time to carefully consider data privacy concerns - with priority on topics of biometrics. Provided careless or too little action is spent to protect the user behind the face image, the more the chance that data may be used by an adversary maliciously [66].

Several have recently attempted to solve problems of bias in demographic-based classifiers (*e.g.*, ethnicity and gender classifiers). Furthermore, attempts to disguise demographic information in facial encodings while preserving FV abilities have been proposed for privacy and protection purposes [67], [68]. In other words, prior works recognized the importance of preserving the identity information in facial features, while ridding it of evidence of demographics. Our model inherently does this as part of the objective aims for an inability to recognize subgroups.

The aforementioned assume the facial encoding are accessible - this makes sense in terms of reduced computations (*i.e.*, no need to encode each time) and storage (*i.e.*, encodings are smaller representations of the image). However, several works aimed to hide attribute information in image space; for instance, Othman *et al.* learned to morph faces to suppress gender information in the image-space while preserving the identification [69]. Guo *et al.* proposed a mapping from image-to-noise, both encrypting the image such that the encoder still decodes the identity but without the ability to determine gender by machine or human [70]. Ma *et al.* viewed the communication between servers as the point of concern for privacy- a lightweight privacy preserving adaptive boosting (AdaBoost) FR framework (POR) based on additive fusion for secret sharing to encrypt model parameters, while using a cascade of classifiers to address different protocols [71].

3 BALANCED FACES IN THE WILD (BFW)

BFW provides balanced data across ethnicity (*i.e.*, Asian (A), Black (B), Indian (I), and White (W)) and gender (*i.e.*, Female (F) and Male (M))— a total of eight demographics referred to as subgroups (Fig. 4). As listed in Table 1, BFW has an equal number of subjects per subgroup (*i.e.*, 100 subjects per subgroup) and faces

per subject (*i.e.*, 25 faces per subject). Note that the key difference between BFW and DemogPairs is in the additional attributes and the increase in overall labeled data; the differences from RFW and FairFace are in the identity labels and distributions (Table 2).

BFW was built with VGG2 [50] by using a set of classifiers on the list of names, and then the corresponding face data. Specifically, we ran a name-ethnicity classifier [72] to generate the initial list of subject proposals. Then, the list was further refined by processing the corresponding faces with ethnicity [73] and gender [74] classifiers. Next, we manually validated, keeping only those that were true members of the respective subgroup. Faces for each subject were then limited to a total of 25 faces that were selected at random, with the distribution of the resolution of the detected faces (*i.e.*, area of the bounding boxes) shown in Fig. 5. Thus, BFW was obtained with minimal human input, having had the proposal lists generated by automatic machinery. We refer the reader to our conference paper for more details [10].

The subgroups of BFW were determined based on physical features most common amongst the respective subgroup [10], which can be regarded as multiple domains due to the feature distributions mismatch across these subgroups. However, the assumption that a discrete label has the capacity to describe an individual is, at best, imprecise. Nonetheless, the assumption allows for a finer-grain analysis of subgroup and is a step in the right direction. Thus, we refute any claim that our efforts here are the final solution; however, we insist that the data and proposed machinery are merely an attempt to establish a foundation for future work to extend. In any case, the two gender for the four ethnic groups make up the eight subgroups of the BFW dataset (Fig. 4). Formally put, the tasks addressed have labels for gender $l^g \in \{F, M\}$ and ethnicity $l^e \in \{A, B, I, W\}$, where the K subgroups (*i.e.*, demographics) are then $K = |l^g| * |l^e| = 8$.

4 METHODOLOGY

To discuss the bias and privacy concerns addressed by the proposed, we first introduce facial verification (FV). Specifically, we review the problem statement, the supporting facial image dataset, along with the objectives of the proposed framework set to achieve the solutions sought in this work. That is to say, to preserve identity information while balancing the sensitivities of encodings for the different demographics (*i.e.*, subgroups), and in a way, to remove knowledge of the subgroups from the facial encoding - the typical representation available for operational cases.

4.1 Problem statement

FV systems make decisions based on the likeliness a pair of faces are of the same identity. In fact, the core procedure of verification systems are often similar to the FR employed for various applications. Specifically, a Convolutional Neural Network (CNN) is trained on a closed set of identities, and then later used to encode faces (*i.e.*, map face images to features). The encodings are then compared in closeness to produce a single score— often via cosine similarity in FR [75]. It is imperative to learn the optimal score threshold separating true from false pairs. The threshold is the decision boundary in score space, *i.e.*, the *matching function*.

4.1.1 The matching function

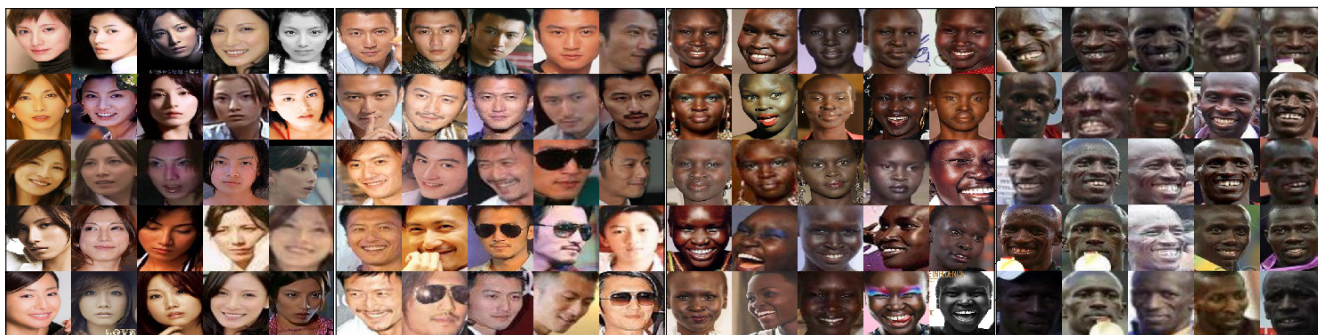
A real-valued similarity score R assumes a discrete label of $Y = 1$ for *genuine* pairs (*i.e.*, a true-match) or $Y = 0$ for *imposter* (*i.e.*, untrue-match). The real-value is mapped to a discrete label

TABLE 1: **BFW features compared to related resources.** Note, the balance across identity (ID), gender (G), and ethnicity (E). Compared with DemogPairs, BFW provides more samples per subject and subgroups per set. Also, BFW uses a single resource, VGG2. RFW; on the other hand, supports a different task (*i.e.*, subgroup classification). Furthermore, RFW and FairFace focus on race-distribution without the support of identity labels.

Database		Number of			Balanced Labels		
Name	Source	Faces	IDs	Subgroups	ID	E	G
RFW [3]	MS-Celeb-1M	≈80,000	≈12,000	4	✗	✓	✗
DemogPairs [52]	CASIA-W, VGG (+2)	10,800	600	6	✓	✓	✓
FairFace [53]	Flickr, Twitter, Web	108,000	–	10	✗	✓	✓
BFW (ours) [10]	VGG2	20,000	800	8	✓	✓	✓

TABLE 2: **Data statistics, nomenclature, and scores for subgroups provided as part of our BFW data.** *Top:* Specifications of BFW and subgroup definitions. *Middle:* Number of pairs for each partition. *Bottom:* Accuracy using a global threshold t_g , the value of the optimal threshold t_o , and accuracy using t_o (bottom) per subgroup. Columns grouped by race and then further split by gender. Notice that ratings are inconsistent across subgroups.

	Asian (A)		Black (B)		Indian (I)		White (W)		Aggregated
	Female (AF)	Male (AM)	BF	BM	IF	IM	WF	WM	
No. Faces	2,500	2,500	2,500	2,500	2,500	2,500	2,500	2,500	20,000
No. Subjects	100	100	100	100	100	100	100	100	800
No. Faces / subject	25	25	25	25	25	25	25	25	25
No. Positive	30,000	30,000	30,000	30,000	30,000	30,000	30,000	30,000	240,000
No. Negative	85,135	85,232	85,016	85,141	85,287	85,152	85,223	85,193	681,379
Total	115,135	115,232	115,016	115,141	115,287	115,152	115,223	115,193	921,379
Acc@ t_g	0.876	0.944	0.934	0.942	0.922	0.949	0.916	0.918	0.925±0.022
t_o	0.235	0.274	0.267	0.254	0.299	0.295	0.242	0.222	0.261±0.025
Acc@ t_o	0.916	0.964	0.955	0.971	0.933	0.958	0.969	0.973	0.955 ± 0.018



(a) Asian-Female (AF). (b) Asian-Male (AM). (c) Black-Female (BF). (d) Black-Male (BM).



(e) Indian-Female (IF). (f) Indian-Male (IM). (g) White-Female (WF). (h) White-Male (WM).

Fig. 4: **Samples of BFW.** For each subgroup, 25 samples for a single, randomly selected subject are shown.

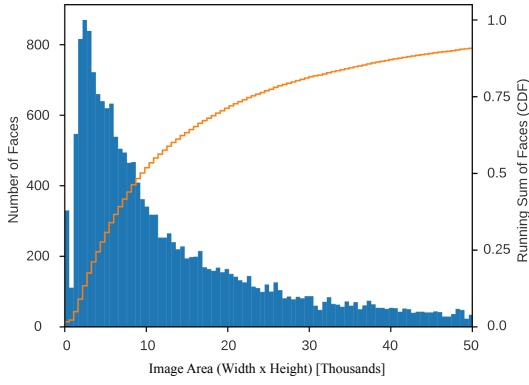


Fig. 5: **BFW statistics (i.e., pixel counts)**. Histogram of image areas in pixels (blue plot). The orange curve shows the cumulative count of images up to a given area.

by $\hat{Y} = \mathbb{I}\{R > \theta\}$ for some predefined threshold θ . The aforementioned can be expressed as *matcher* d operating as

$$f_{boolean}(\vec{x}_i, \vec{x}_j) = d(\vec{x}_i, \vec{x}_j) \leq \theta, \quad (1)$$

where the face encodings in \vec{x} being the i^{th} and j^{th} sample—a conventional scheme in the FR research communities [77]. We use cosine similarity as the *matcher* in Eq. 1, which produces a score in closeness for the i^{th} and j^{th} faces (i.e., l -th face pair) by $d(\vec{x}_i, \vec{x}_j) = s_l = \frac{f_i \cdot f_j}{\|f_i\|_2 \|f_j\|_2}$. The decision boundary formed by threshold θ controls the level of *acceptance* and *rejection*. Thus, θ inherits a trade-off between the sensitivity and specificity. The operating point chosen is done so, most always, depending on the purpose of the respective system (i.e., perhaps higher sensitivity (or lower threshold) for threat-related tasks, in that flagging a few extra is worth not overlooking the one true positive). Specifically, the trade-off involves FNR, a Type 1 Error where *genuine* attempts to pass but is falsely rejected. Mathematically, it relates by

$$\text{FNR} = \frac{\text{FN}}{\text{P}} = \frac{\text{FN}}{\text{FN} + \text{TP}} = 1 - \text{TAR} = 1 - \frac{\text{TP}}{\text{FN} + \text{TP}},$$

with positive counts P, true-positive (TP), and false-negative (FN).

The other error type contributes to the FPR, is referred to as the Type II Error as an *imposter*, and is falsely accepted:

$$\text{FAR} = \frac{\text{FP}}{\text{N}} = \frac{\text{FP}}{\text{FP} + \text{TN}} = 1 - \text{TNR} = 1 - \frac{\text{TN}}{\text{FP} + \text{TN}},$$

where the counts negatives is N, and the metrics are true-negative (TN), false-positive (FP), true-negative rate (TNR), and FAR. A *matching* function is the module typically characterized using the listed metrics (Fig 1). The geometric relationships of the metrics related to the score distributions and the choice in threshold show the trade-offs in error rates (Fig. 2).

The hyperparameter θ is often determined for a desired error rate on a held-out validation, and is use-case specific. In research, it is typically set to acquire the best performance possible. Some analyze θ as a range of values, for a more complete characterization is often obtainable with evaluation curves that inherently show performance trade-offs. However, the held-out validation and test sets typically share data distributions as a single source partitioned into subsets (i.e., train, validation, test). Regardless, the decision boundary in score space that maximizes the performance is transferred to the pin-point (i.e., 1D) decision

boundary - in our case, with cosine similarity, the value is a floating point value spanning [0, 1].

4.1.2 Feature alignment

Domain \mathcal{D} can be represented by the tuple $\mathcal{D} = \{(\mathbf{x}_i, y_i) \in \mathcal{X} \times \mathcal{Y}\}_{i=1}^N$, with \mathcal{X} and \mathcal{Y} representing the input feature space and output label space, respectively. The objective of FR algorithms is to learn a mapping function (i.e., an hypothesis): $\eta : \mathcal{X} \rightarrow \mathcal{Y}$, which assigns each sample vector with a semantic identity label.

In domain adaptation, a model is trained on source data and deployed on target data, where an abundance of paired data is available to train a model for a task similar to that of the target. Mathematically, the labeled source domain \mathcal{D}_S and the unlabeled target domain \mathcal{D}_T can be denoted as $\mathcal{D}_S = \{(\mathbf{x}_i^s, y_i^s) \in \mathcal{X}_S \times \mathcal{Y}_S\}_{i=1}^{N_S}$ and $\mathcal{D}_T = \{\mathbf{x}_i^t \in \mathcal{X}_T\}_{i=1}^{N_T}$ with the sample count $N_S = |\mathcal{D}_S|$ and $N_T = |\mathcal{D}_T|$ corresponding to the i -th sample (i.e., $\mathbf{x}_i \in \mathbb{R}^d$) and label (i.e., $y_i \in \{1, \dots, K\}$). \mathcal{D}_S and \mathcal{D}_T are further defined by tasks \mathcal{T}_S and \mathcal{T}_T , which is indicative of the exact label type(s) and the specific K classes of interest. The goal is to learn an objective $\eta_S : \mathcal{X}_S \rightarrow \mathcal{Y}_S$, and then transfer to target \mathcal{D}_T for \mathcal{T}_T . By this, knowledge is leveraged from both \mathcal{D}_S for \mathcal{D}_T , with the goal of obtaining η_T . Since such two domains share different marginal distributions, i.e., $p(\mathbf{x}^s) \neq p(\mathbf{x}^t)$, as well as distinct conditional distributions, i.e., $p(y^t|\mathbf{x}^t) \neq p(y^t|\mathbf{x}^s)$, the model trained only by the labeled source domain samples usually performs poorly on the unlabeled target domain. A typical solution towards such domain gap is to learn a model f that aligns the features in a shared subspace: $p(f(\mathbf{x}^s)) \approx p(f(\mathbf{x}^t))$.

4.2 Proposed framework

Given samples with identity and subgroup labels— $\mathcal{D} = \{\mathbf{x}_i, y_i^{id}, y_i^{att}\}_{i=1}^N$, where $\mathbf{x} \in \mathbb{R}^d$, $y^{id} \in \{1, \dots, I\}$ and $y^{att} \in \{1, \dots, K\}$ — are used for the two objectives of the proposed framework (Fig. 6). Hence, we aim to learn a mapping $\mathbf{f}_{deb} = M(\mathbf{x}, \Theta_M)$ to a lower dimensional space $\mathbf{f}_{deb} \in \mathbb{R}^{d/2}$ that preserves identity information of the target. This is dubbed the identity loss \mathcal{L}_{ID} . We also learn to do so without subgroup information, which we call the attribute (or subgroup) loss \mathcal{L}_{ATT} . The total loss (i.e., the final objective $\mathcal{L} = \mathcal{L}_{ID} + \mathcal{L}_{ATT}$) is formed by summing the two aforementioned loss functions:

$$\mathcal{L}_{ID} = -\frac{1}{N} \sum_{i=1}^N \sum_{k=1}^I \mathbf{1}_{[k=y_i^{id}]} \log(p(y = y_i^{id}|\mathbf{x}_i)), \quad (2)$$

$$\mathcal{L}_{ATT} = -\frac{1}{N} \sum_{i=1}^N \sum_{k=1}^K \mathbf{1}_{[k=y_i^{att}]} \log(p(y = y_i^{att}|\mathbf{x}_i)), \quad (3)$$

where $p(y = y_i^{id}|\mathbf{x}_i)$ and $p(y = y_i^{att}|\mathbf{x}_i)$ represent the softmax conditional probability of its identity and attribute.

We added \mathcal{L}_{ATT} to debias the features to remove variation in scores that were previously handled with a variable threshold. Further, a byproduct are these features that preserve identity information without containing knowledge of subgroup—a critical concern in the privacy and protection of biometric data.

There are three groups of parameters (i.e., Θ_M , Θ_{ID} and Θ_{ATT}) required to be optimized by the objective (Fig. 6). Both the identity classifier C_{ID} and attribute classifier C_{ATT} are used to find a feature space that remains accurate to identity and not for subgroup by minimizing the empirical risk of \mathcal{L}_{ID} and \mathcal{L}_{ATT} :

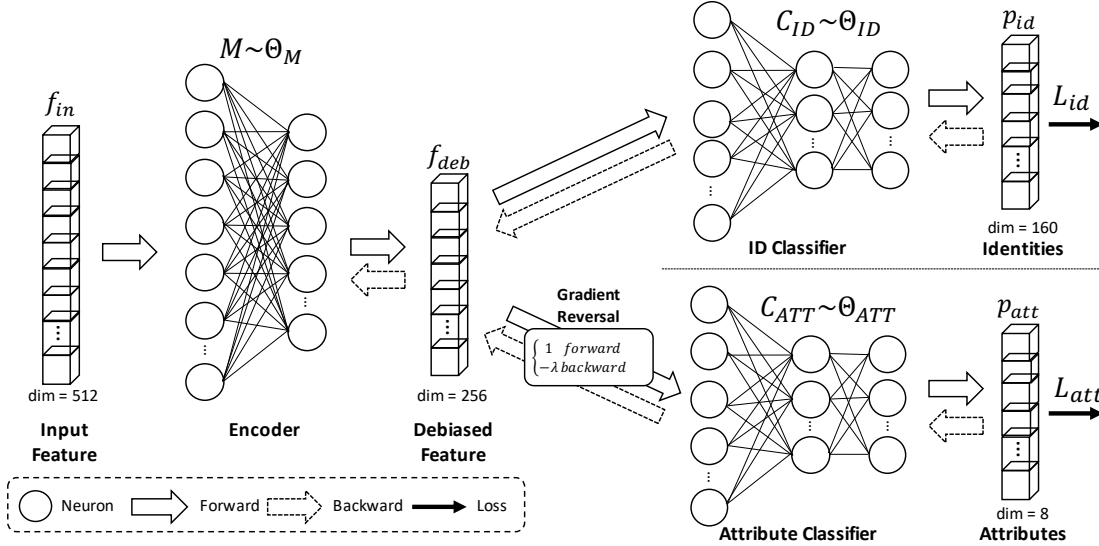


Fig. 6: **Debiasing framework.** The framework used to learn a projection that casts facial encodings to a space that (1) preserves identity information (*i.e.*, C_{ID}) and (2) removes knowledge of subgroup (*i.e.*, C_{ATT}). The benefits of this are two-fold: ability to verify pairs of faces fairly across attributes and an inability to classify attribute for privacy and safety purposes. Note, that the *gradient reversal* [76] flips the sign of the error back-propagated from C_{ATT} to M by scalar λ during training.

$$\Theta_{ID}^* = \arg \min_{\Theta_{ID}} \mathcal{L}_{ID}, \tag{4}$$

$$\Theta_{ATT}^* = \arg \min_{\Theta_{ATT}} \mathcal{L}_{ATT}. \tag{5}$$

It is important to note that the task of \mathcal{L}_{ATT} is to be incorrect (*i.e.*, learn a mapping that contains no knowledge of subgroup). Thus, a gradient reversal layer [76] that acts as the identity during the forward pass, while inverting the sign of the gradient back-propagated with a scalar λ as the adversarial loss during training:

$$\Theta_M^* = \arg \min_{\Theta_M} -\lambda \mathcal{L}_{ATT} + \mathcal{L}_{ID}. \tag{6}$$

Although the proposed learning scheme is simple, it proved effective for both objectives we seek to solve. The effectiveness is clearly demonstrated in the results and analysis.

5 EXPERIMENTS

Two sets of experiments are done to demonstrate the effectiveness of the proposed using our balanced BFW [10]. First, we evaluate verification performance using debiasing. Specifically, we compare the reported results compared to the actual results per subgroup. Then, for the privacy preserving claim, we compare the performance of models trained on top of debiased features f_{deb} with those of the original features f_{in} . For each, we present the problem statement, metrics and settings, and analysis. Finally, we do an ablation study to show the performance on the renowned LFW benchmark [77].

5.1 Common settings

The baseline (*i.e.*, f_{in}) were encoded using Arcface [8] (*i.e.*, ResNet-34).² MS1M [48] was the train set, providing about 5.8M faces for 85k subjects. We prepared the faces using MTCNN [78]

to detect five facial landmarks. A similarity transformation then was applied to align the face by the five detected landmarks, from which we cropped and resized each to 96×112 . The RGB (*i.e.*, pixel values of $[0, 255]$) were normalized by centering about 0 (*i.e.*, subtracting 127.5) and then standardizing (*i.e.*, dividing by 128); encodings were later L2 normalized [79]. The batch size was 200, and a stochastic gradient descent optimizer with a momentum 0.9, weight decay $5e-4$, and learning rate started at 0.1 and decreased by a factor of 10 two times when the error leveled. The choice in these settings was made based on Arcface being among the best performing FR deep models to date, and as it has become a popular choice for an *off-the-shelf* option for face recognition technology and applications.

For all experiments we used our BFW dataset (Section 3): the debias and privacy-based experiments use the predefined five-folds³; the ablation study on LFW uses all of BFW to train M (Fig. 6). As mentioned, BFW was built using data of VGG2, and there exist no overlap with CASIA-Webface and LFW used to train the face encoder and for the ablation, respectfully.

5.2 Debias experiment

Typical FR systems are graded by the percent error - whether to a customer, prospective staff, and so forth. In other words, specialized curves, confusion matrices, and other metrics are not always the best way to communicate system performances to non-technical audiences. It is better to discuss ratings in a manner that is more globally understood, and more comprehensible with respect to the use-case. A prime example is to share the error rate per number correctly. For instance, claiming that a system predicts 1 FP per 10,000 predictions. However, such an approximation can be hazardous, for it is inherently misleading. To demonstrate this, we ask the following questions. *Does this claim hold true for different demographics? Does this rating depend on the types of faces - does it hold for all males or all females?* Thus, if we set

2. <https://github.com/deepinsight/insightface>

3. <https://github.com/visionjo/facerec-bias-bfw>

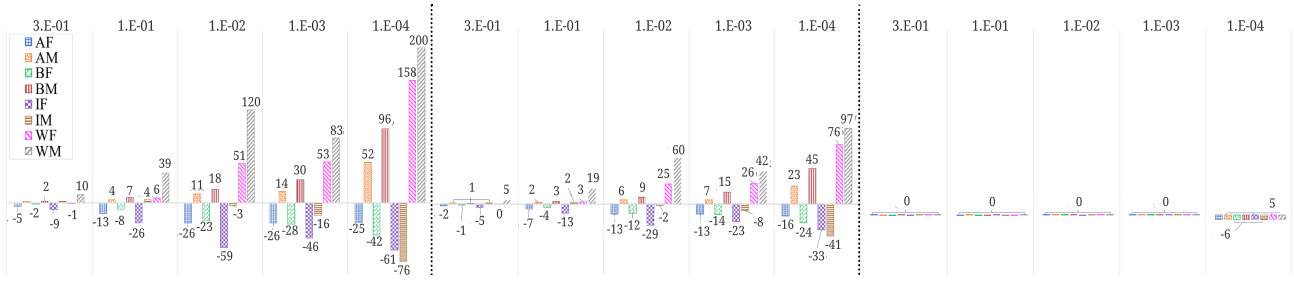


Fig. 7: **Percent difference from intended FPR as a function of subgroup.** *Left:* global threshold (t_g) yields a FPR that spans up to 200% the intended (*i.e.*, WM for $1e-4$); the F subgroups tend to perform worse than intended for all, while M’s overshoot the intended performances besides IM at $FPR=1e-4$. *Right:* Subgroup-specific (or optimal) thresholds t_o reduces the difference closer to zero. Furthermore, the proposed method (*middle*), which does not assume knowledge of attribute information at inference like for t_o , clearly mitigates the issue of the inconsistencies in the true versus reported FPR. Similar to the results in Table 3, the variations are nearly halved: the percent difference for subgroups is more balanced using the features adapted with our approach versus the baseline.

our system according to a desired FAR, would the claim be fair regardless of demographics (*i.e.*, subgroups) of population.

The aforementioned questions were central to our previous work [10]. We found the answer to these questions to be clear - *No, the report FAR is not true when analyzed per subgroup.* We found when comparing the FAR values (*i.e.*, the reported-to-the-actual), the values drastically deviate from the reported average when the score threshold is fixed for all subgroups. Furthermore, demographic-specific thresholds, meaning an assumption that demographic information is known prior, proved to mitigate the problem. However, prior knowledge of demographic, although plausible (*e.g.*, identifying a known subject on a *black list*), it is a strong assumption that limits the practical uses for which it could be deployed. To extend our prior work, we propose a debiasing scheme to reduce the differences between the reported and actual. In other words, we set out to make the claim in reported false rates to be fair across all involved demographics.

5.2.1 Metrics and settings

TAR and FAR are used to examine the trade-off in the confusions that is dependent on the choice of threshold discussed earlier. Specifically, we look at actual TAR scores as a function of desired FAR. Furthermore, we compute the following metric, the percent difference of the true and reported FAR values (*i.e.*, an average score is targeted). So we ask, *how well do the different subgroups compare to that average?* Specifically,

$$\% \text{ Error}(l) = \left(\frac{\text{FAR}(l)_{\text{reported}} - \text{FAR}(l)_{\text{actual}}}{\text{FAR}(l)_{\text{reported}}} \right) * 100\% \quad (7)$$

5.2.2 Analysis

The proposed balances results in a way that significantly boosts the TAR at a given FAR. The percent difference between in reported to actual FAR score implies a more fair representation has been acquired Fig. 7: left-most are the percent differences using a single threshold and the right-most is using a variable threshold (*i.e.*, results of [10]). The proposed adaptation scheme did not only preserve performances, and with a slight boost (Table 3), but comparing the actual to the shows a smoothing out in deviations.

Several hard positives that were incorrectly classified by the baseline but correctly identified by the proposed are shown in Fig. 8. The set was selected for having scores closest to the

global threshold of the baseline. Also, the sample pairs shown were correctly matched by the proposed. Notice the quality of one or more of the faces in each pairs is often low-resolution; additionally, extreme pose differences between faces of each pair also is common. These challenges are overcome by the proposed scheme - mitigating the issue of bias boosts results, and there displayed are several of the pairs that went from falsely being rejected to correctly being accepted.

5.3 Privacy preserving experiment

As mentioned, our objective was two-fold. First, we aimed to preserve identity information while debiasing the facial features, as demonstrated in the prior experiment. But then, secondly, our objective function injected the reverse gradient as part of the loss to force the embedding to be unable to classify subgroups (*i.e.*, demographics). In other words, another benefit of the proposed debiasing scheme is that it rids the facial encodings of demographic information. This, in itself, is of interest in problems of privacy and protection - ideally, face encodings, which often are the only representation of face information available at the system level, will not include attribute information, like gender or ethnicity. Hence, we aim for the inability to learn subgroup classifiers on top of the features as a means to show the demographic information has been reduced.

To show the effectiveness of the proposed in removing subgroup information, we train a multi-layered perception (MLP) to classify subgroups on top of the features. We can then measure the amount of information present in the face representation [28].

The MLP designed in Keras as follows: three fully-connected layers of size 512, 512, and 256 fed into the output fully-connected layer (*i.e.*, size 8 for the 8 subgroup classes). The first three layers were separated by ReLU activation and drop-out [80] (*i.e.*, probability of 0.5) while only dropout (again, 0.5) was place prior to the output softmax layer. A categorical crossentropy loss with Adam [81] set with a learning rate of $1e-3$ was used to train.

5.3.1 Metrics and settings

We will examine the overall accuracy of the subgroup classifiers by use of a confusion matrix. Specifically, we will look at how often each subgroup was predicted correct and, when incorrect, the percentage it was mistaken for the others. The confusion was generated by averaging across the five folds.

TABLE 3: **TAR at intervals of FAR.** TAR scores for a global threshold (top), the proposed debiasing transformation (middle), optimal threshold (bottom). Higher is better. The standard deviation from the average is shown to demonstrate the standard error comparing the reported (*i.e.*, average) to the subgroup-specific scores. The proposed recovers most of the loss from using a global threshold rather than a per-subgroup threshold.

FAR	0.3	0.1	0.01	0.001	0.0001
AF	0.990	0.867	0.516	0.470	0.465
	0.996	0.874	0.521	0.475	0.470
	1.000	0.882	0.524	0.478	0.474
AM	0.994	0.883	0.529	0.482	0.477
	0.996	0.886	0.531	0.484	0.479
	1.000	0.890	0.533	0.486	0.482
BF	0.991	0.870	0.524	0.479	0.473
	0.995	0.875	0.527	0.481	0.476
	1.000	0.879	0.530	0.484	0.480
BM	0.992	0.881	0.526	0.480	0.474
	0.995	0.886	0.529	0.483	0.478
	1.000	0.891	0.532	0.485	0.480
IF	0.996	0.881	0.532	0.486	0.481
	0.998	0.883	0.533	0.487	0.483
	1.000	0.884	0.534	0.488	0.484
IM	0.997	0.895	0.533	0.485	0.479
	0.998	0.897	0.534	0.486	0.480
	1.000	0.898	0.535	0.486	0.481
WF	0.988	0.878	0.517	0.469	0.464
	0.992	0.884	0.522	0.472	0.468
	1.000	0.894	0.526	0.478	0.474
WM	0.989	0.896	0.527	0.476	0.470
	0.996	0.901	0.530	0.479	0.474
	1.000	0.910	0.535	0.483	0.478
Std. Dev.	0.030	0.010	0.006	0.006	0.006
	0.002	0.009	0.005	0.005	0.005
	0.000	0.010	0.004	0.004	0.004
Avg.	0.992	0.881	0.526	0.478	0.473
	0.998	0.886	0.528	0.481	0.476
	1.000	0.891	0.531	0.483	0.479

Besides accuracy and confusions, we examine the precision and recall for each of the subgroups, along with the overall average. Precision, a measure of time correct when the prediction assumed to be true, is calculated as follows:

$$P(l) = \frac{TP}{TP + FP}, \tag{8}$$

where the average precision (AP) is the mean of all subgroups $l \in L$ (*i.e.*, $|L| = P_L$) for a given true-positive rate (TPR).

The recall R, which is the ratio of the number of predicted-to-actual positive samples, is found as

$$R(l) = \frac{TP}{TP + FN}. \tag{9}$$

This compliments the confusion by allowing the specificity and sensitivity of the subgroups to also be examined. Nonetheless, there are inherent trade-offs between P and R. This motivates the F_1 -score [82], which fuses P and R as the harmonic mean,

$$F_1 = 2 * \frac{P * R}{P + R}. \tag{10}$$

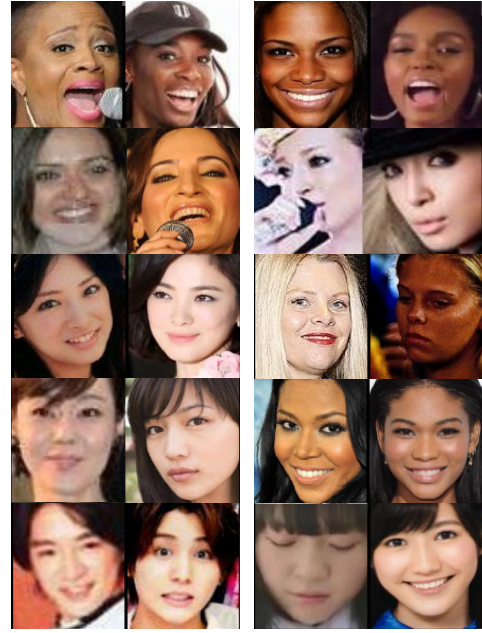


Fig. 8: **Sample pairs of hard positives.** Pairs incorrectly classified by the baseline and correctly matched by the proposed.

5.3.2 Analysis

We demonstrated that identity knowledge is preserved (Table 3), and now we show the other benefits in privacy. The results clearly show that the privacy preserving claim is accurate, leading to a 30% drop in the ability to predict gender and ethnicity from the encodings (Table 4). Hence, predictive power of all subgroups dropped significantly. Furthermore, the drop in performance is sufficient enough to make the claim that the predictions are now unreliable. Honing in on the specifics, it is interesting to note that the subgroups for which the baseline were most in favor of are hindered the most from the debias scheme. In other words, WM and WF drop the most, while the AM and AF drop the least. All the while the same trends in confusions propagate from the baseline to the proposed results. For instance, WM are mostly confused as IM originally, and then again in the case for the debiased features. The same holds for the opposite sex in all cases.

Next, we examine the confusions for the different subgroups before and after debiasing the face features (Fig. 9). As established, the baseline contains more subgroup knowledge— a

TABLE 4: **Subgroup classification results.** The baseline and proposed are on the left and right columns, respectively. Note that the columns on the right have lower scores as intended.

	Precision		Recall		F1	
AF	0.962	0.734	0.927	0.852	0.943	0.788
AM	0.864	0.707	0.974	0.730	0.915	0.717
BF	0.940	0.655	0.924	0.644	0.932	0.647
BM	0.961	0.644	0.962	0.668	0.961	0.653
IF	0.961	0.641	0.935	0.649	0.948	0.644
IM	0.898	0.519	0.902	0.589	0.898	0.550
WF	0.934	0.554	0.970	0.547	0.951	0.549
WM	0.943	0.524	0.848	0.317	0.892	0.392
Average	0.933	0.622	0.930	0.624	0.930	0.617

AF	92.7	7.0	0.0	0.0	0.1	0.0	0.2	0.0
AM	1.6	97.4	0.1	0.1	0.0	0.2	0.0	0.7
BF	0.8	0.0	92.4	2.8	0.9	0.0	3.0	0.0
BM	0.0	0.0	2.0	96.2	0.0	1.6	0.0	0.2
IF	0.9	0.0	3.0	0.0	93.5	0.4	2.2	0.0
IM	0.0	3.6	0.0	0.8	2.0	90.2	0.0	3.3
WF	0.4	0.4	0.8	0.0	0.4	0.0	97.0	1.1
WM	0.0	4.6	0.0	0.1	0.3	8.6	1.6	84.8
	AF	AM	BF	BM	IF	IM	WF	WM

(a) Baseline subgroup classifier.

AF	85.2	8.8	1.1	0.3	1.7	0.6	1.5	1.0
AM	10.2	73.0	3.1	1.2	1.6	3.8	4.6	2.6
BF	3.5	3.8	64.4	11.4	5.4	3.2	6.5	1.8
BM	1.5	2.1	13.3	66.8	4.5	5.7	4.0	2.1
IF	2.2	2.3	4.6	5.7	64.9	13.9	4.2	2.2
IM	1.7	3.7	1.4	5.4	9.9	58.9	8.4	10.6
WF	1.4	4.5	5.2	7.9	5.8	11.7	54.7	8.8
WM	10.4	5.4	6.1	6.0	7.9	17.1	15.4	31.7
	AF	AM	BF	BM	IF	IM	WF	WM

(b) Our subgroup classifier.

Fig. 9: **Subgroup confusion matrix.** Comparison of accuracy in classifying and misclassifying the subgroups. Notice the (b) performs significantly worse than (a) as intended.

model can learn on top. When trained and evaluated on BFW, the baseline performs better on F subgroups. This differs from the norm where M are a majority of the data. To the contrary, the WM are inferior in performances to all subgroups in either case.

5.4 Ablation study

To check the effectiveness of the proposed scheme we train M using the entire BFW dataset and deploy on the well-known LFW benchmark. We note that the training dataset that we employ is significantly smaller than that used by SOTA networks trained to achieve high performance on LFW, which employ the MS1MV2 dataset, which contains 5.8M images of 85k identities. By contrast, even though we initialize our network starting with features learnt on MS1MV2, we train on a small dataset of 20k images of 800 subjects, which is two orders of magnitude smaller. Although we train the current SOTA with 99.8% verification accuracy, while the proposed scheme reaches its best score of 95.2% after 5 epochs before dropping off and then leveling out around 81% (Fig. 10). Clearly, the benefits of privacy and debiasing are hindered on

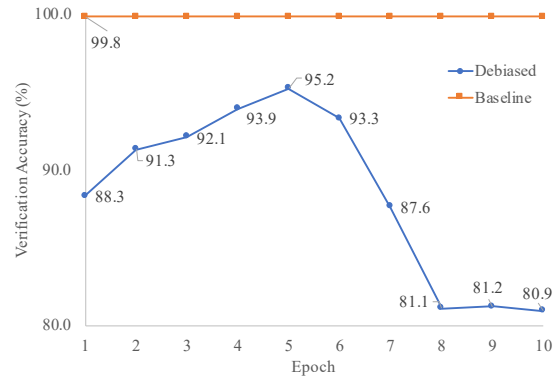


Fig. 10: **Accuracy on LFW benchmark.** The proposed approaches the performance of the baseline before dropping off.

unbalanced data (*i.e.*, LFW is made up of about 85% WM). Furthermore, we optimized M by choosing the epoch with the best performance prior to the drop off. Future steps could be improving the proposed when transferring to unbalanced sets with a way to detect the optimal training settings.

6 CONCLUSION AND FUTURE WORK

We show a bias for subgroups in FR caused by the selection of a single threshold. Previously, a subgroup-specific threshold was proposed as a solution for the case in which such knowledge (*i.e.*, subgroup information) is accessible prior. Inspired by works in feature alignment and domain adaptation we propose a scheme to mitigate the bias problem. We learn a lower dimensional mapping that preserves identity and removes knowledge of subgroup. The encodings balance the performance across subgroups, while boosting the overall accuracy. Using a single threshold, the difference between actual and average performance across subgroups is reduced. Furthermore, the resulting encodings hold reduced knowledge of subgroups, increasing privacy.

REFERENCES

- [1] A. Acien, A. Morales, R. Vera-Rodriguez, I. Bartolome, and J. Fierrez, "Measuring the gender and ethnicity bias in deep models for face recognition," in *Progress in Pattern Recognition, Image Analysis, Computer Vision, and Applications*, R. Vera-Rodriguez, J. Fierrez, and A. Morales, Eds. Springer International Publishing, 2019. 1
- [2] L. Anne Hendricks, K. Burns, K. Saenko, T. Darrell, and A. Rohrbach, "Women also snowboard: Overcoming bias in captioning models," in *Proceedings of the European Conference on Computer Vision*, 2018. 1
- [3] M. Wang, W. Deng, J. Hu, J. Peng, X. Tao, and Y. Huang, "Race faces in-the-wild: Reduce bias by deep unsupervised domain adaptation," *CoRR arXiv:1812.00194*, 2019. 1, 3, 5
- [4] C. Lazo, "Towards engineering ai software for fairness: A framework to help design fair, accountable and transparent algorithmic decision-making systems," *TU Delft Library*, 2020. 1
- [5] P. Drozdowski, C. Rathgeb, A. Dantcheva, N. Damer, and C. Busch, "Demographic bias in biometrics: A survey on an emerging challenge," *IEEE Transactions on Technology and Society*, 2020. 1, 2, 3
- [6] J. Deng, J. Guo, N. Xue, and S. Zafeiriou, "Arcface: Additive angular margin loss for deep face recognition," in *IEEE Conference on Computer Vision and Pattern Recognition (CVPR)*, 2019. 1, 2
- [7] W. Liu, Y. Wen, Z. Yu, M. Li, B. Raj, and L. Song, "Sphereface: Deep hypersphere embedding for face recognition," in *IEEE Conference on Computer Vision and Pattern Recognition (CVPR)*, 2017. 1, 2
- [8] F. Wang, J. Cheng, W. Liu, and H. Liu, "Additive margin softmax for face verification," *IEEE Signal Processing Letters*, 2018. 1, 7
- [9] H. Wang, Y. Wang, Z. Zhou, X. Ji, D. Gong, J. Zhou, Z. Li, and W. Liu, "Cosface: Large margin cosine loss for deep face recognition," in *IEEE Conference on Computer Vision and Pattern Recognition*, 2018. 1

- [10] J. P. Robinson, G. Livitz, Y. Henon, C. Qin, Y. Fu, and S. Timoner, "Face recognition: too bias, or not too bias?" in *Computer Vision and Pattern Recognition Workshop*, 2020, pp. 0–1. [2, 3, 4, 5, 7, 8](#)
- [11] Y. Taigman, M. Yang, M. Ranzato, and L. Wolf, "Deepface: Closing the gap to human-level performance in face verification," in *IEEE Conference on Computer Vision and Pattern Recognition (CVPR)*, 2014. [2](#)
- [12] O. M. Parkhi, A. Vedaldi, and A. Zisserman, "Deep face recognition," in *British Machine Vision Conference (BMVC)*, 2015. [2](#)
- [13] Y. Wen, K. Zhang, Z. Li, and Y. Qiao, "A discriminative feature learning approach for deep face recognition," in *European Conference on Computer Vision*, 2016, pp. 499–515. [2](#)
- [14] Y. Duan, J. Lu, and J. Zhou, "Uniformface: Learning deep equidistributed representation for face recognition," in *IEEE Conference on Computer Vision and Pattern Recognition (CVPR)*, 2019, pp. 3415–3424. [2](#)
- [15] Z. Wang, G. Wang, B. Huang, Z. Xiong, Q. Hong, H. Wu, P. Yi, K. Jiang, N. Wang, Y. Pei *et al.*, "Masked face recognition dataset and application," *CoRR arXiv:2003.09093*, 2020. [2](#)
- [16] G. Guo and N. Zhang, "A survey on deep learning based face recognition," *Computer Vision and Image Understanding*, 2019. [2](#)
- [17] I. Masi, Y. Wu, T. Hassner, and P. Natarajan, "Deep face recognition: A survey," in *2018 31st SIBGRAPI conference on graphics, patterns and images (SIBGRAPI)*. IEEE, 2018, pp. 471–478. [2](#)
- [18] A. Khalil, S. G. Ahmed, A. M. Khattak, and N. Al-Qirim, "Investigating bias in facial analysis systems: A systematic review," *IEEE Access*, vol. 8, pp. 130 751–130 761, 2020. [2](#)
- [19] M. Merler, N. Ratha, R. S. Feris, and J. R. Smith, "Diversity in faces," *CoRR arXiv:1901.10436*, 2019. [2, 3](#)
- [20] G. Balakrishnan, Y. Xiong, W. Xia, and P. Perona, "Towards causal benchmarking of bias in face analysis algorithms," *CoRR arXiv:2007.06570*, 2020. [3](#)
- [21] M. Georgopoulos, J. Oldfield, M. A. Nicolaou, Y. Panagakis, and M. Pantic, "Enhancing facial data diversity with style-based face aging," in *Computer Vision and Pattern Recognition Workshop*, 2020. [3](#)
- [22] P. Terhörst, J. N. Kolf, N. Damer, F. Kirchbuchner, and A. Kuijper, "Post-comparison mitigation of demographic bias in face recognition using fair score normalization," *CoRR arXiv:2002.03592*, 2020. [3](#)
- [23] I. Serna, A. Peña, A. Morales, and J. Fierrez, "Insidebias: Measuring bias in deep networks and application to face gender biometrics," *CoRR arXiv:2004.06592*, 2020. [3](#)
- [24] V. Albiero, K. KS, K. Vangara, K. Zhang, M. C. King, and K. W. Bowyer, "Analysis of gender inequality in face recognition accuracy," in *Computer Vision and Pattern Recognition Workshop*, 2020, pp. 81–89. [3](#)
- [25] A. Das, A. Dantcheva, and F. Bremond, "Mitigating bias in gender, age and ethnicity classification: a multi-task convolution neural network approach," in *European Conference on Computer Vision*, 2018. [3](#)
- [26] N. Srinivas, K. Ricanek, D. Michalski, D. S. Bolme, and M. King, "Face recognition algorithm bias: Performance differences on images of children and adults," in *Computer Vision and Pattern Recognition Workshop*, 2019. [3](#)
- [27] S. Nagpal, M. Singh, R. Singh, M. Vatsa, and N. Ratha, "Deep learning for face recognition: Pride or prejudiced?" *CoRR arXiv:1904.01219*, 2019. [3](#)
- [28] A. Acien, A. Morales, R. Vera-Rodriguez, I. Bartolome, and J. Fierrez, "Measuring the gender and ethnicity bias in deep models for face recognition," in *Iberoamerican Congress on Pattern Recognition*. Springer, 2018. [3, 8](#)
- [29] S. Gong, X. Liu, and A. K. Jain, "Debface: De-biasing face recognition," *CoRR arXiv:1911.08080*, 2019. [3](#)
- [30] A. V. Savchenko, "Efficient facial representations for age, gender and identity recognition in organizing photo albums using multi-output convnet," *PeerJ Computer Science*, vol. 5, p. e197, 2019. [3](#)
- [31] S. Nagpal, M. Singh, R. Singh, and M. Vatsa, "Attribute aware filter-drop for bias invariant classification," in *Computer Vision and Pattern Recognition Workshop*, June 2020. [3](#)
- [32] T. Sixta, J. Junior, C. Jacques, P. Buch-Cardona, E. Vazquez, and S. Escalera, "Fairface challenge at eccv 2020: Analyzing bias in face recognition," *CoRR arXiv:2009.07838*, 2020. [3](#)
- [33] A. Peña, I. Serna, A. Morales, and J. Fierrez, "Bias in multimodal ai: Testbed for fair automatic recruitment," *CoRR arXiv:2004.07173*, 2020. [3](#)
- [34] —, "Faircvtest demo: Understanding bias in multimodal learning with testbed in fair automatic recruitment," *CoRR arXiv:2009.07025*, 2020. [3](#)
- [35] P. Terhörst, N. Damer, F. Kirchbuchner, and A. Kuijper, "Suppressing gender and age in face templates using incremental variable elimination," in *2019 International Conference on Biometrics (ICB)*, 2019, pp. 1–8. [3](#)
- [36] B. Sadeghi and V. N. Boddeti, "Imparting fairness to pre-trained biased representations," in *Computer Vision and Pattern Recognition Workshop*, June 2020. [3](#)
- [37] M. Wang and W. Deng, "Mitigating bias in face recognition using skewness-aware reinforcement learning," in *IEEE Conference on Computer Vision and Pattern Recognition (CVPR)*, 2020. [3](#)
- [38] P.-M. Law, S. Malik, F. Du, and M. Sinha, "Designing tools for semi-automated detection of machine learning biases: An interview study," *CoRR arXiv:2003.07680*, 2020. [3](#)
- [39] C. Drummond, R. C. Holte *et al.*, "C4. 5, class imbalance, and cost sensitivity: why under-sampling beats over-sampling," in *Workshop on learning from imbalanced datasets II*. Citeseer, 2003. [3](#)
- [40] M. Oquab, L. Bottou, I. Laptev, and J. Sivic, "Learning and transferring mid-level image representations using convolutional neural networks," in *IEEE Conference on Computer Vision and Pattern Recognition (CVPR)*, 2014, pp. 1717–1724. [3](#)
- [41] E. M. Rudd, M. Günther, and T. E. Boult, "Moon: A mixed objective optimization network for the recognition of facial attributes," in *European Conference on Computer Vision*. Springer, 2016, pp. 19–35. [3](#)
- [42] C. Huang, Y. Li, C. L. Chen, and X. Tang, "Deep imbalanced learning for face recognition and attribute prediction," *IEEE Transactions on Pattern Analysis and Machine Intelligence (TPAMI)*, 2019. [3](#)
- [43] H. He and E. A. Garcia, "Learning from imbalanced data," *IEEE Transactions on knowledge and data engineering*, 2009. [3](#)
- [44] H. He and Y. Ma, *Imbalanced learning: foundations, algorithms, and applications*. John Wiley & Sons, 2013. [3](#)
- [45] B. Krawczyk, "Learning from imbalanced data: open challenges and future directions," *Progress in Artificial Intelligence*, 2016. [3](#)
- [46] T. Xu, J. White, S. Kalkan, and H. Gunes, "Investigating bias and fairness in facial expression recognition," *CoRR arXiv:2007.10075*, 2020. [3](#)
- [47] V. Albiero, K. Zhang, and K. W. Bowyer, "How does gender balance in training data affect face recognition accuracy?" *CoRR arXiv:2002.02934*, 2020. [3](#)
- [48] Y. Guo, L. Zhang, Y. Hu, X. He, and J. Gao, "Ms-celeb-1m: A dataset and benchmark for large-scale face recognition," in *European Conference on Computer Vision*, 2016. [3, 7](#)
- [49] F. Schroff, D. Kalenichenko, and J. Philbin, "Facenet: A unified embedding for face recognition and clustering," in *IEEE Conference on Computer Vision and Pattern Recognition (CVPR)*, 2015, pp. 815–823. [3](#)
- [50] Q. Cao, L. Shen, W. Xie, O. M. Parkhi, and A. Zisserman, "Vggface2: A dataset for recognising faces across pose and age," in *IEEE International Conference on Automatic Face and Gesture Recognition*, 2018. [3, 4](#)
- [51] B. Maze, J. Adams, J. A. Duncan, N. Kalka, T. Miller, C. Otto, A. K. Jain, W. T. Niggel, J. Anderson, J. Cheney *et al.*, "Iarpa janus benchmark-c: Face dataset and protocol," in *2018 International Conference on Biometrics (ICB)*. IEEE, 2018, pp. 158–165. [3](#)
- [52] I. Hupont and C. Fernández, "Demogpairs: Quantifying the impact of demographic imbalance in deep face recognition," in *IEEE International Conference on Automatic Face and Gesture Recognition (FG)*. IEEE, 2019, pp. 1–7. [3, 5](#)
- [53] K. Kärkkäinen and J. Joo, "Fairface: Face attribute dataset for balanced race, gender, and age," *CoRR arXiv:1908.04913*, 2019. [3, 5](#)
- [54] D. Yi, Z. Lei, S. Liao, and S. Z. Li, "Learning face representation from scratch," *CoRR arXiv:1411.7923*, 2014. [3](#)
- [55] Z. Ding, S. Li, M. Shao, and Y. Fu, "Graph adaptive knowledge transfer for unsupervised domain adaptation," in *ECCV*, 2018. [3](#)
- [56] X. Peng, B. Usman, N. Kaushik, J. Hoffman, D. Wang, and K. Saenko, "Visda: The visual domain adaptation challenge," *CoRR arXiv:1710.06924*, 2017. [3](#)
- [57] K. Saito, D. Kim, S. Sclaroff, T. Darrell, and K. Saenko, "Semi-supervised domain adaptation via minimax entropy," *CoRR arXiv:1904.06487*, 2019. [3, 4](#)
- [58] R. Shu, H. H. Bui, H. Narui, and S. Ermon, "A dirt-t approach to unsupervised domain adaptation," *CoRR arXiv:1802.08735*, 2018. [3, 4](#)
- [59] B. Sun and K. Saenko, "Subspace distribution alignment for unsupervised domain adaptation," in *BMVC*, 2015. [4](#)
- [60] M. Long, J. Wang, G. Ding, J. Sun, and P. S. Yu, "Transfer feature learning with joint distribution adaptation," in *ICCV*, 2013. [4](#)
- [61] B. Gong, Y. Shi, F. Sha, and K. Grauman, "Geodesic flow kernel for unsupervised domain adaptation," in *CVPR*, 2012. [4](#)
- [62] R. Gopalan, R. Li, and R. Chellappa, "Domain adaptation for object recognition: An unsupervised approach," in *ICCV*, 2011. [4](#)
- [63] Y. Ganin, E. Ustinova, H. Ajakan, P. Germain, H. Larochelle, F. Laviolette, M. Marchand, and V. Lempitsky, "Domain-adversarial training of neural networks," *JMLR*, vol. 17, no. 1, 2016. [4](#)
- [64] E. Tzeng, J. Hoffman, K. Saenko, and T. Darrell, "Adversarial discriminative domain adaptation," in *CVPR*, 2017. [4](#)

[65] B. Güler, A. S. Avestimehr, and A. Ortega, "Privacy-aware distributed graph-based semi-supervised learning," in *International Workshop on Machine Learning for Signal Processing*. IEEE, 2019. 4

[66] K. W. Bowyer, "Face recognition technology: security versus privacy," *IEEE Technology and society magazine*, vol. 23, no. 1, pp. 9–19, 2004. 4

[67] P. Dhar, J. Gleason, H. Souri, C. D. Castillo, and R. Chellappa, "An adversarial learning algorithm for mitigating gender bias in face recognition," *CoRR arXiv:2006.07845*, 2020. 4

[68] V. Mirjalili, S. Raschka, and A. Ross, "Gender privacy: An ensemble of semi adversarial networks for confounding arbitrary gender classifiers," in *2018 IEEE 9th International Conference on Biometrics Theory, Applications and Systems (BTAS)*, 2018, pp. 1–10. 4

[69] A. Othman and A. Ross, "Privacy of facial soft biometrics: Suppressing gender but retaining identity," in *Computer Vision - ECCV 2014 Workshops*, L. Agapito, M. M. Bronstein, and C. Rother, Eds. Cham: Springer International Publishing, 2015, pp. 682–696. 4

[70] S. Guo, T. Xiang, and X. Li, "Towards efficient privacy-preserving face recognition in the cloud," *Signal Processing*, vol. 164, pp. 320 – 328, 2019. [Online]. Available: <http://www.sciencedirect.com/science/article/pii/S0165168419302324> 4

[71] Z. Ma, Y. Liu, X. Liu, J. Ma, and K. Ren, "Lightweight privacy-preserving ensemble classification for face recognition," *IEEE Internet of Things Journal*, vol. 6, no. 3, pp. 5778–5790, 2019. 4

[72] A. Ambekar, C. Ward, J. Mohammed, S. Male, and S. Skiena, "Name-ethnicity classification from open sources," in *Proceedings of SIGKDD conference on Knowledge Discovery and Data Mining*, 2009. 4

[73] S. Fu, H. He, and Z.-G. Hou, "Learning race from face: A survey," *IEEE Transactions on Pattern Analysis and Machine Intelligence (TPAMI)*, 2014. 4

[74] G. Levi and T. Hassner, "Age and gender classification using convolutional neural networks," in *Computer Vision and Pattern Recognition Workshop*, 2015, pp. 34–42. 4

[75] H. V. Nguyen and L. Bai, "Cosine similarity metric learning for face verification," in *Asian Conference on Computer Vision (ACCV)*. Springer, 2010, pp. 709–720. 4

[76] Y. Ganin and V. Lempitsky, "Unsupervised domain adaptation by backpropagation," in *International Conference on Machine Learning (ICML)*. PMLR, 2015, pp. 1180–1189. 7

[77] G. B. Huang, M. Ramesh, T. Berg, and E. Learned-Miller, "Labeled faces in the wild: A database for studying face recognition in unconstrained environments," U. of Massachusetts, Amherst, Tech. Rep., 2007. 6, 7

[78] K. Zhang, Z. Zhang, Z. Li, and Y. Qiao, "Joint face detection and alignment using multitask cascaded convolutional networks," *Signal Processing Letters*, 2016. 7

[79] F. Wang, X. Xiang, J. Cheng, and A. L. Yuille, "Normface: L2 hypersphere embedding for face verification," in *ACM Conference on Multimedia*, 2017, pp. 1041–1049. 7

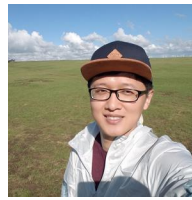
[80] N. Srivastava, G. Hinton, A. Krizhevsky, I. Sutskever, and R. Salakhutdinov, "Dropout: a simple way to prevent neural networks from overfitting," *The journal of machine learning research*, vol. 15, no. 1, pp. 1929–1958, 2014. 8

[81] D. P. Kingma and J. Ba, "Adam: A method for stochastic optimization," *CoRR arXiv:1412.6980*, 2014. 8

[82] L. A. Jeni, J. F. Cohn, and F. De La Torre, "Facing imbalanced data—recommendations for the use of performance metrics," in *Humaine association conference on affective computing and intelligent interaction*. IEEE, 2013, pp. 245–251. 9



Joseph P Robinson Received a B.S. in electrical & computer engineering (2014) and Ph.D. in computer engineering (2020) at Northeastern University, where he was also part-time faculty: designed and taught Data Analytics (2020 *Best Teacher*). Research is in applied machine vision, with emphasis on faces, deep learning, MM, big data. Previously, led a team to TRECVID debut (MED, 3rd-place). Built many image and video datasets— most notably FIW. Organizing chair of the 2020 FG conference, various workshops and challenges (e.g., NECV, RFIW, AMFG, FacesMM), tutorials (MM, CVPR, FG), PC (e.g., CVPR, FG, MIRP, MMEDIA, AAAI, ICCV), reviewer (e.g., IEEE TBioCAS, TIP, TPAMI), and positions like President of IEEE@NEU (adviser as grad student) and Relations Officer of IEEE SAC R1 Region. Completed: NSF REUs (2010 & 2011); interned at Analog Corporation (2012) and BBN Technology (2013), MIT Lincoln Labs (2014), System & Technology Research (2016 & 2017), Snap Inc. (2018), ISMConnect (2019).



has published at top-tier conferences (i.e., NeurIPS, AAAI, ECCV).

Can Qin Received the B.E. from the School of Microelectronics, Xidian University, China (2018), and is pursuing a Ph.D. at the Department of Electrical and Computer Engineering, Northeastern University, under Dr. Yun Raymond Fu. His research focus spans transfer learning, semi-supervised learning, and deep learning in broad. He received awards for the *Best Paper Award* of the Real-World Recognition from *Low-Quality Images and Videos* workshop at 2019 ICCV. Additionally, he

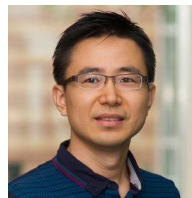


Yann Henon received a B.S. and an M.S from Monash University in Melbourne, Australia. His research has focused on medical imaging and has been published in top journals including *Developmental Cell*, *Journal of Applied Physiology* and *RSC Advances*.



facial detection and recognition algorithms.

Samson Timoner received a B.S. in Applied Physics from Caltech (1997), and a Ph.D. in Electrical Engineering and Computer Science From MIT (2003). Samson has organized numerous workshops including CVPR View, CVPR ProCams, the New Computer Vision Workshop. Samson has started two computer vision companies. He is an organizer of the computer vision community in Boston, bringing researchers and entrepreneurs together. He is currently Principal Scientist at ISM focusing on



Science at Northeastern University since 2012. His research interests are Machine Learning, Computational Intelligence, Big Data Mining, Computer Vision, Pattern Recognition, and Cyber-Physical Systems. He has extensive publications in leading journals, books/book chapters and international conferences/workshops. He serves as associate editor, chairs, PC member and reviewer of many top journals and international conferences/workshops. He received seven Prestigious Young Investigator Awards from NAE, ONR, ARO, IEEE, INNS, UIUC, Grainger Foundation; eleven Best Paper Awards from IEEE, ACM, IAPR, SPIE, SIAM; many major Industrial Research Awards from Google, Samsung, Amazon, Konica Minolta, JP Morgan, Zebra, Adobe, and Mathworks, etc. He is currently an Associate Editor of the IEEE Transactions on Neural Networks and Learning Systems. He is fellow of IEEE, IAPR, OSA and SPIE, a Lifetime Distinguished Member of ACM, Lifetime Member of AAAI, and Institute of Mathematical Statistics, member of Global Young Academy, INNS and Beckman Graduate Fellow during 2007-2008.

Yun Fu (S'07-M'08-SM'11-F'19) received the B.Eng. degree in information engineering and the M.Eng. degree in pattern recognition and intelligence systems from Xi'an Jiaotong University, China, respectively, and the M.S. degree in statistics and the Ph.D. degree in electrical and computer engineering from the University of Illinois at Urbana-Champaign, respectively. He is an interdisciplinary faculty member affiliated with College of Engineering and the College of Computer and Information